RIS-Aided Unsourced Random Access

Mohammad Javad Ahmadi, Mohammad Kazemi and Tolga M. Duman
Department of Electrical and Electronics Engineering
Bilkent University, Ankara, Turkey
{ahmadi, kazemi, duman}@ee.bilkent.edu.tr

Abstract—**This paper considers an unsourced random access (URA) set-up equipped with a passive reconfigurable intelligent surface (RIS), where a massive number of unidentified users (of which only a small fraction are active at a given time) share the same communication resources. Employing RIS can improve the performance of the URA system by creating additional links between the base station (BS) and the users located in blind areas. We propose a slotted transmission scheme that operates in two phases. In the first phase, called the RIS configuration phase, the base station detects active pilots and estimates their respective channel state information. Then, using the estimated channel coefficients, the base station suitably selects the phase shifts of the RIS elements. In the second phase, called the data phase, transmitted messages of active users are decoded. The proposed channel estimator offers the capability to estimate the channel coefficients of multiple users whose pilots interfere with each other without access to the list of selected pilots or the number of active users. We show that the proposed RIS phase-shift design is well suited to the URA scenario where the direct link between the users and the BS is completely blocked. The effectiveness of the proposed algorithms is confirmed through computer simulations.**

I. Introduction

Unsourced random access (URA) is an important paradigm to support applications such as Internet-of-things (IoT), where a large number of users with small payloads share a common codebook and a common frame to sporadically transmit their signals to a base station (BS) [1]. Under this framework, the BS cares only about the transmitted messages, i.e., the identity of users is not important, and the per-user probability of error (PUPE) is used as the performance criterion. Many coding schemes have been devised for URA over a Gaussian multiple-access channel (GMAC) [2]–[4], and block-fading channels [5]–[8].

Reconfigurable intelligent surface (RIS) is a promising technology developed for providing high spectral efficiency and energy savings for 5G and beyond wireless communication systems. Specifically, a passive RIS equipped with many low-cost passive elements, which can intelligently tune the phase-shift of the incident electromagnetic waves, and reflect them in a desired direction without any amplification, can improve the efficiency of the network by enabling line-of-sight paths between the transmitters and the receivers in problematic environments with many blocking obstacles [9]–[15].

URA schemes in the literature consider direct links between all the users and the BS [1]–[8]; however, in practice, the direct link between some users and the BS may be blocked or significantly attenuated. Therefore, the use of RIS can improve user connectivity in URA by creating high-quality links between the BS and the users.

One of the most crucial problems in RIS-aided communication systems is the design of RIS reflecting coefficients to achieve the best system performance. This is solved via various approaches, e.g., alternating optimization algorithm [9], [10], Gaussian randomization [11], [12], gradient descent approach [13], and semidefinite relaxation technique [14]. To design the RIS elements, a reliable knowledge of channel state information (CSI) is required. For this purpose, many grant-based schemes solve the channel estimation problem in a multi-user system by providing each user an individual time slot [15]–[21]. Specifically, they assign each user an orthogonal pilot so that their CSI can be estimated without suffering from interference due to the simultaneous transmission of other users. However, orthogonal transmission is not feasible in the URA set-up, hence new solutions are needed.

In this paper, we propose a slotted URA scheme facilitated by a passive RIS coupled with the necessary channel estimation, RIS design, and pilot and data detection algorithms. The proposed scheme operates in two phases: the RIS configuration phase and the data phase. The RIS configuration phase is responsible for jointly detecting the active pilots and estimating the CSI via the newly proposed joint detection and channel estimation algorithm (JDCE), as well as designing the reflection coefficients of the RIS elements. During the data phase, the actual data transmission takes place. As stated above, unlike the grant-based schemes, where each identified user's CSI is estimated without suffering from interfering pilots of other users, in URA, signals from multiple users interfere with each other due to the unsourced nature of transmission for which there is no cooperation between the users and the BS, or among the users themselves. Therefore, conventional channel estimators are not efficient since CSI estimation is not a straightforward task. However, the proposed JDCE algorithm is able to perform channel estimation in the presence of interference without any prior knowledge of the number of active users and their transmitted pilots. In the proposed RIS-aided URA set-up, in addition, we need to design the RIS reflection coefficients. On the other hand, for the encoder and decoder designs, similar solutions with other URA schemes can be adopted [5], [6]. In particular, in this paper, we employ polar codes along with successive interference cancellation (SIC) for the data phase to recover the transmitted messages.

This research is funded by the Scientific and Technological Research Council of Turkey (TUBITAK) under grant 119E589.

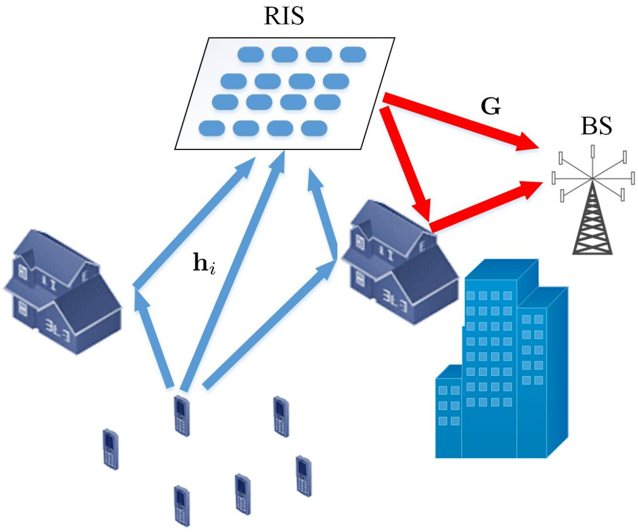

Fig. 1: Illustration of a RIS-aided URA system where the direct link between the users and the BS is obstructed.

The paper is organized as follows. In Section II, we describe the system model. In Section III, the encoding and decoding structures of the proposed RIS-aided URA scheme are introduced. We provide simulation results in Section IV, and conclude the paper in Section V.

Notation: Lower-case and upper-case boldface letters are used to denote a vector and a matrix, respectively; $\mathrm{diag}(\mathbf{t})$ and $\mathbf{I}_N$ represent a diagonal matrix with elements of vector $\mathbf{t}$ in its diagonal, and an $N\times N$ identity matrix, respectively; $\mathrm{Re}(\cdot)$ and $\mathrm{trace}(\cdot)$ denote the real part and trace of a matrix, respectively; $[\mathbf{T}]_{(i,j)}$ refers to the element in the ith row and jth column of $\mathbf{T}$; $\mathrm{vec}(\cdot)$ is the vectorization operator; $\otimes$ denotes the Kronecker product; $\mathcal{CN}(\mathbf{0},\mathbf{B})$ denotes the zero-mean circularly symmetric complex Gaussian random variable with covariance matrix $\mathbf{B}$; $U(c,d)$ is the continuous uniform distribution on $[c,d]$; and, the set $\mathcal{F}(N)=\{-1,-1+\Delta_N,-1+2\Delta_N,-1+3\Delta_N,...,-1-(N-1)\Delta_N\}$ with $\Delta_N=2/N$.

II. System Model

Consider a RIS-aided URA system as depicted in Fig. 1, where a BS with M receive antennas serves K_T single-antenna users (of which only K_a of them are active in any transmission frame) with the help of a passive N-element RIS. We assume that both the BS and the RIS are equipped with a uniform planer array (UPA) [16]. Active users send B bits of information to the BS through n channel uses. Employing the Saleh-Valenzuela channel model, the RIS-BS channel is written as [11]

$$\mathbf{G}=\sqrt{MN}\sum_{l=1}^{L_G}\mu_l\mathbf{a}_M(\phi_{r,l},\psi_{r,l})^T\mathbf{a}_N(\phi_{t,l},\psi_{t,l})\in\mathbb{C}^{M\times N}, \tag{1}$$

where $(\phi_{r,l},\psi_{r,l})$ are the azimuth and elevation angles of arrival (AOA) at the BS from the lth path, $(\phi_{t,l},\psi_{t,l})$ are the azimuth and elevation angles of departure (AOD) from the RIS to the BS through the lth path, L_G is the number of paths from RIS to the BS, μ_l denotes the lth path's gain which is modeled as $\mu_l\sim\mathcal{CN}(0,C_0 d_l^{\alpha_0})$ [22], d_l is the length of the lth path, C_0 and α_0 denote the path loss at the reference distance and path loss exponent, and $\mathbf{a}_N(\phi,\psi)$ is the array steering vector of an $N_1\times N_2$ UPA ($N=N_1N_2$) which is represented as [1]

$$\mathbf{a}_N(\phi,\psi)=\bar{\mathbf{a}}_{N,\bar{\phi},\bar{\psi}}=\frac{1}{\sqrt{N}}e^{-j2\pi\bar{\phi}\mathbf{n}_1}\otimes e^{-j2\pi\bar{\psi}\mathbf{n}_2}\in\mathbb{C}^{1\times N}, \tag{2}$$

where $\mathbf{n}_1=\frac{d}{\lambda}[0,...,N_1-1]$, $\mathbf{n}_2=\frac{d}{\lambda}[0,...,N_2-1]$, $\bar{\phi}=\sin(\phi)\cos(\psi)$, $\bar{\psi}=\sin(\psi)$, λ denotes the carrier wavelength, and d is the antenna spacing. Note also that $\mathbf{a}_M(\phi,\psi)$ is the array steering vector of an $M_1\times M_2$ UPA ($M=M_1M_2$) which is obtained by replacing N by M in (2). Similarly, the channel from the ith user to the RIS can be expressed as

$$\mathbf{h}_i=\sqrt{N}\sum_{f_i=1}^{L_i}\mu_{f_i}\mathbf{a}_N(\phi_{i,f_i},\psi_{i,f_i})\in\mathbb{C}^{1\times N}, \tag{3}$$

where L_i is the number of paths between the ith user and the RIS, $(\phi_{i,f_i},\psi_{i,f_i})$ are azimuth and elevation AOAs at the RIS for the f_ith path of the ith user's signal, with the distance d_{f_i} and the corresponding path gain μ_{f_i}(the path-loss model is the same as in the RIS-BS channel). The channel between the RIS and the BS is assumed to be perfectly known. This can be justified by the fact that the RIS and the BS are stationary, so the channel between them changes very slowly, and it can be well estimated with negligible overhead. Therefore, it is enough to focus on the estimation of the channel between each user and the RIS for our set-up.

Let $\mathbf{y}_t\in\mathbb{C}^{M\times 1}$ denote the uplink signal received at the BS at time t. Assuming that the direct link between the users and the BS is completely blocked, and the channel coefficients are constant throughout the frame, the received signal can be written as [16]

$$\mathbf{y}_t=\sum_{i=1}^{K_a}\mathbf{G}\mathrm{diag}(\mathbf{h}_i)\mathbf{w}_t x_{i,t}+\mathbf{z}_t,\in\mathbb{C}^{M\times 1},\ t=1,...,n, \tag{4}$$

where $\mathbf{w}_t\in\mathbb{C}^{N\times 1}$ denotes the reflection coefficient vector of the RIS at time t with $\left|[\mathbf{w}_t]_{(i,1)}\right|=1$ (passive RIS assumption), $x_{i,t}\in\mathbb{C}$ is the symbol transmitted by the ith user at time t, and $\mathbf{z}_t\sim\mathcal{CN}(\mathbf{0},\sigma_z^2\mathbf{I}_M)$ represents the noise vector at time t.

III. The Proposed RIS-aided URA scheme

The proposed coding scheme divides the entire frame into slots. Each active user randomly selects only one slot to transmit its pilot and data signals in two parts as illustrated in Fig. 2. At the receiver side, transmitted messages are decoded in two phases: RIS configuration and data phases. In the RIS configuration phase, active pilots in each slot are identified, and the corresponding CSI between the users and the RIS is estimated. Given the estimated channel of each active user, the BS designs the RIS reflection coefficients,

[1]For the vector $\mathbf{t}$, we denote the element-wise exponentiation by $e^{\mathbf{t}}$.

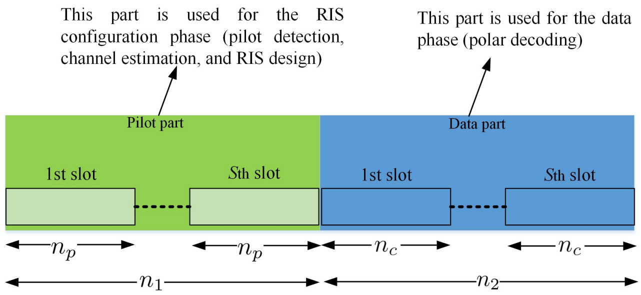

Fig. 2: Transmission scheme of the proposed URA scheme.

and transmits them back to the RIS unit. After the phases of the RIS elements are adjusted accordingly, the set of active users transmits their encoded signals in the data transmission phase. We describe the adopted encoder and decoder structures in more detail in the following.

A. Encoder

As shown in Fig. 2, a length-n frame is divided into pilot and data parts with lengths n_1 and n_2, respectively, where $n_2 + n_1 = n$. We also divide each part into S slots of lengths $n_p = n_1/S$ and $n_c = n_2/S$. The ith user divides its B bits of information into two groups: pilot part $\omega_{pi} \in \{0,1\}^{1\times B_p}$ and data part $\omega_{ci} \in \{0,1\}^{1\times B_c}$, where $B = B_p + B_c$. Every user obtains a preamble $\mathbf{b}_i \in \mathbb{C}^{1\times n_s}$ and a pilot $\mathbf{p}_i \in \mathbb{C}^{1\times n_p}$ by mapping ω_{pi} to the rows of the preamble codebook $\mathbf{B} \in \mathbb{C}^{2^{B_p}\times n_s}$ and the pilot codebook $\mathbf{P} \in \mathbb{C}^{2^{B_p}\times n_p}$, respectively. The ith user adds cyclic redundancy check (CRC) bits to ω_{ci}, and encodes the result with an $(n_d,\ B_c + r)$ polar code. The encoded bits are then modulated using binary phase-shift keying (BPSK), which results in $\mathbf{v}_i = [v_{i,1}, v_{i,2}, ...v_{i,n_d}] \in \{\pm 1\}^{1\times n_d}$, where r is the number of CRC bits. To construct the signal of the data part, the encoder spreads each symbol of the modulated signal by its preamble [3], [4], i.e., $\mathbf{c}_i = \mathbf{v}_i \otimes \mathbf{b}_i \in \mathbb{C}^{1\times n_c}$, where $n_c = n_s n_d$. The ith user randomly selects a slot index (denoted by ζ_i), and transmits $\mathbf{p}_i$ and $\mathbf{c}_i$ through the ζ_ith slot of the pilot and data parts, respectively.

Using the signal model in (4), the received signal at the sth slot of the pilot part can be written as

$$\mathbf{Y}_p = \sqrt{P_p} \sum_{i\in\mathcal{S}_s} \mathbf{G}\mathrm{diag}(\mathbf{h}_i)\mathbf{W}_{p_s}\mathrm{diag}(\mathbf{p}_i) + \mathbf{Z}_p \in \mathbb{C}^{M\times n_p}, \tag{5}$$

where P_p denotes the signal power in the data part, $\mathcal{S}_s$ is the set of users in the sth slot, $\mathbf{W}_{p_s} = [\mathbf{w}_{j_{1,s}}, ..., \mathbf{w}_{j_{n_p,s}}]$ contains the RIS reflecting coefficients in the sth slot of the pilot part (which is arbitrarily set), $\mathbf{Z}_p = [\mathbf{z}_{j_{1,s}}, ..., \mathbf{z}_{j_{n_p,s}}]$, and $j_{t,s} = (s-1)n_p + t$. We omit the slot index from matrices for notational simplicity. Similarly, the received signal at the sth slot of the data part corresponding to the fth ($f = 1, 2, ..., n_c$) symbol of the modulated signal can be written as

$$\mathbf{Y}_{c,f} = \sqrt{P_c} \sum_{i\in\mathcal{S}_s} \mathbf{G}\mathrm{diag}(\mathbf{h}_i)\mathbf{W}_{c_s}\mathrm{diag}(\mathbf{b}_i)v_{i,f} + \mathbf{Z}_{c,f} \in \mathbb{C}^{M\times n_s}, \tag{6}$$

where P_c denotes the signal power in the data part, $\mathbf{W}_{c_s} = [\mathbf{w}_{k_{1,s}}, ..., \mathbf{w}_{k_{n_s,s}}]$ contains the RIS reflecting coefficients in the sth slot of the data part, $\mathbf{Z}_{c,f} = [\mathbf{z}_{k_{1,s}}, ..., \mathbf{z}_{k_{n_s,s}}]$, and $k_{t,s} = Sn_p + (s-1)n_c + (f-1)n_s + t$.

B. Decoder

1) Joint Pilot Detection and Channel Estimation: In the following, we describe the steps of JDCE algorithm. It is clear from (3) that detecting all the active paths (finding angles of active paths), and estimating the corresponding path gains give us an estimate of the user-RIS channel $\mathbf{h}_i$. In the proposed JDCE algorithm, the pilot with the highest probability of existence is detected first, then the strongest path over which the detected pilot arrives at the RIS is identified. We also estimate the gain corresponding to the detected path using the least-squares (LS) technique. Finally, we remove the contribution of the detected pilot-path pair from the received signal, and repeat the procedure on the remaining signal to detect the next pilot-path pair. Note that since the received signal is updated at each iteration, we denote it by $\mathbf{Y}_p^j$, where j is the iteration index. Details of the proposed JDCE algorithm are described below:

- **Step 1** (pilot detection): the pilot with the highest probability of existence is detected using the energy detection approach as in [3], [4]
$$\hat{k} = \underset{k\in 1,2,...,2^{B_p}}{\arg\max}\ \mathrm{trace}(\mathbf{Q}_k\mathbf{R}_{pj}\mathbf{Q}_k^H), \tag{7}$$
where $\mathbf{R}_{pj} = \mathbf{Y}_p^{j\,H}\mathbf{Y}_p^j$, $\mathbf{Q}_k = \mathbf{W}_{p_s}\mathrm{diag}(\bar{\mathbf{p}}_k)$, and $\bar{\mathbf{p}}_k$ is the kth row of the codebook $\mathbf{P}$.
- **Step 2** (path detection): By solving the following problem, we find the strongest path through which the $\hat{k}$th pilot (the detected pilot) arrives at the RIS
$$(\hat{l}, \hat{q}) = \underset{l\in\mathcal{F}(N_1), q\in\mathcal{F}(N_2)}{\arg\max} \frac{\mathrm{trace}(\mathbf{F}_{l,q}\mathbf{R}_{pj}\mathbf{F}_{l,q}^H)}{\mathrm{trace}(\mathbf{F}_{l,q}\mathbf{F}_{l,q}^H)}, \tag{8}$$
where $\mathbf{F}_{l,q} = \mathbf{G}\mathrm{diag}(\bar{\mathbf{a}}_{N,l,q})\mathbf{W}_{p_s}\mathrm{diag}(\bar{\mathbf{p}}_{\hat{k}})$, and $\bar{\mathbf{a}}_{N,l,q}$ is defined in (2).
- **Step 3** (SIC): from (5), we can infer that the contribution of the received signal corresponding to the detected pilot-path pair in the jth iteration can be obtained as
$$\mathbf{U}_j = \sqrt{P_p}\mathbf{G}\mathrm{diag}(\bar{\mathbf{a}}_{N,\hat{l},\hat{q}})\mathbf{W}_{p_s}\mathrm{diag}(\bar{\mathbf{p}}_{\hat{k}}) \in \mathbb{C}^{M\times n_p}. \tag{9}$$
Vectorizing both sides of (5), the received signal vector at the initial iteration ($\mathbf{y}_p^1 = \mathrm{vec}(\mathbf{Y}_p^1) \in \mathbb{C}^{Mn_p\times 1}$) can be written as
$$\mathbf{y}_p^1 = \sum_{j'=1}^{j} m_{j'}\mathbf{u}_{j'} + \mathbf{z}'_p, \tag{10}$$
where $\mathbf{u}_j = \mathrm{vec}(\mathbf{U}_j) \in \mathbb{C}^{Mn_p\times 1}$, $m_{j'} \in \mathbb{C}$ is the path gain corresponding to the pilot-path pair detected at the j'th iteration, and $\mathbf{z}'_p \in \mathbb{C}^{Mn_p\times 1}$ contains the signals corresponding to the pilot-path pairs that are not detected yet along with the vectorized noise term.

The path gains can be estimated using LS as

$$\hat{\mathbf{m}} = (\bar{\mathbf{U}}^H\bar{\mathbf{U}})^{-1}\bar{\mathbf{U}}^H\mathbf{y}_p^1, \tag{11}$$

where the kth column of $\bar{\mathbf{U}} \in \mathbb{C}^{Mn_p\times j}$ is $\mathbf{u}_k$. Then, the contribution of $\bar{\mathbf{U}}$ is removed from the initially received signal to obtain

$$\mathbf{y}_p^{(j+1)} = \mathbf{y}_p^1 - \bar{\mathbf{U}}\hat{\mathbf{m}}. \tag{12}$$

Finally, $\mathbf{y}_p^{(j+1)}$ is converted back to an $M \times n_p$ matrix $\mathbf{Y}_p^{(j+1)}$ before being passed to Step 1 for the $(j+1)$th iteration. The procedure is stopped if conditions $\|\mathbf{y}_p^{(j+1)}\|^2/\|\mathbf{y}_p^j\|^2 > \alpha_1$ and $\|\mathbf{y}_p^j\|^2/\|\mathbf{y}_p^{(j-1)}\|^2 > \alpha_1$ are satisfied, where $\alpha_1 \in \mathbb{R}^+$ is a threshold.

2) Data Phase: We now devise an iterative algorithm to detect the data part of the message (ω_{ci}) using the received signal in the data part. The algorithm 1) generates log-likelihood ratios (LLRs) of the polar coded bits using the estimated channel coefficients, 2) passes the LLRs to the polar list decoder, 3) removes the contribution of the successfully decoded users (users whose detected messages satisfy the CRC check) from the received signal. The remaining received signal is passed back to the first step to generate a new LLR. The algorithm is repeated until no message is successfully decoded during an iteration. Details of the proposed algorithm are given below:
We can rewrite the received signal in (6) as

$$\mathbf{Y}_{c,f} = \sum_{i\in\mathcal{S}_s}\mathbf{T}_i v_{i,f} + \mathbf{Z}_{c,f}, \tag{13}$$

where $\mathbf{T}_i = \sqrt{P_c}\mathbf{G}\text{diag}(\mathbf{h}_i)\mathbf{W}_{c_s}\text{diag}(\mathbf{b}_i) \in \mathbb{C}^{M\times n_s}$. Vectorizing both sides of (13), we write

$$\begin{aligned}\mathbf{y}_{c,f} &= \sum_{i\in\mathcal{S}_s}\mathbf{t}_i v_{i,f} + \mathbf{z}_{c,f}\\ &= \bar{\mathbf{T}}\tilde{\mathbf{v}}_f + \mathbf{z}_{c,f},\end{aligned} \tag{14}$$

where $\mathbf{y}_{c,f} = \text{vec}(\mathbf{Y}_{c,f}) \in \mathbb{C}^{Mn_s\times 1}$, $\mathbf{t}_i = \text{vec}(\mathbf{T}_i) \in \mathbb{C}^{Mn_s\times 1}$, $\mathbf{z}_{c,f} = \text{vec}(\mathbf{Z}_{c,f}) \in \mathbb{C}^{Mn_s\times 1}$, $v_{i,t}$ is the ith row of $\tilde{\mathbf{v}}_f \in \mathbb{C}^{|\mathcal{S}_s|\times 1}$, and $\mathbf{t}_i$ is the ith column of $\bar{\mathbf{T}} \in \mathbb{C}^{Mn_s\times|\mathcal{S}_s|}$. We estimate $\tilde{\mathbf{v}}_f$ using the minimum mean square error (MMSE) estimator as

$$\hat{\mathbf{v}}_f = [\hat{v}_{1,f}, \hat{v}_{2,f}, ..., \hat{v}_{|\mathcal{S}_s|,f}]^T = \bar{\mathbf{T}}^H\hat{\mathbf{R}}^{-1}\mathbf{y}_{c,f}, \tag{15}$$

where

$$\hat{\mathbf{R}} = \mathbb{E}\{\mathbf{y}_{c,f}\mathbf{y}_{c,f}^H\} = \bar{\mathbf{T}}\bar{\mathbf{T}}^H + \sigma_z^2\mathbf{I}_{Mn_s}. \tag{16}$$

Similarly as in [3], the LLR of the fth symbol of the ith user is constructed as

$$\hat{g}_{i,f} = 2\text{Re}\left(\hat{v}_{i,f}/\delta_i\right), \tag{17}$$

where δ_i is the ith diagonal element of the matrix $\mathbf{\Sigma} = \mathbf{I}_{|\mathcal{S}_s|} - \bar{\mathbf{T}}^H\hat{\mathbf{R}}^{-1}\bar{\mathbf{T}}$. The LLR values obtained are passed to the polar list decoder.

Finally, the contribution of users whose decoded message sequences satisfy the CRC check is removed from the received signal employing

$$\mathbf{Y}_{c,f} = \mathbf{Y}_{c,f} - \mathbf{T}_i\bar{v}_{i,f}, \tag{18}$$

where $\bar{v}_{i,f}$ is the fth symbol of the ith user obtained by encoding and modulating its successfully decoded message. The remaining signal $\mathbf{Y}_{c,f}$ is passed back to the MMSE estimator in (15) for the next iteration. The iterations are stopped if no user is successfully decoded during an iteration.

3) RIS Design: We now propose an iterative algorithm for designing the RIS phase-shift matrix for use in the data part, $\mathbf{W}_{c_s}$. Note that since the RIS is designed based on the decoder, we introduce it after studying the data phase of the decoder. However, in practice, RIS design is performed before data transmission.

We know from Section III-B2 that the MMSE estimate of the BPSK signal is fed to the polar decoder. Thus, improving the signal-to-interference-plus-noise ratio (SINR) at the output of the MMSE block is a good way to decrease the decoding error of each user. Plugging (14) into (15), we can obtain the MMSE estimate at the fth symbol of the ith user's codeword as

$$\hat{v}_{i,f} = \mathbf{t}_i^H\hat{\mathbf{R}}^{-1}\mathbf{t}_i v_{i,f} + \mathbf{t}_i^H\hat{\mathbf{R}}^{-1}\left(\sum_{k\in\mathcal{S}_s,k\neq i}\mathbf{t}_i v_{k,f} + \mathbf{z}_{p,f}\right), \tag{19}$$

where the first and second terms are signal and interference-plus-noise terms, respectively, whose powers can be computed as

$$\begin{aligned}\sigma_{s,i}^2 &= \mathbb{E}\{\|\mathbf{t}_i^H\hat{\mathbf{R}}^{-1}\mathbf{t}_i v_{i,f}\|^2\}\\ &= (\mathbf{t}_i^H\hat{\mathbf{R}}^{-1}\mathbf{t}_i)^2,\end{aligned} \tag{20}$$

$$\begin{aligned}\sigma_{\text{IN},i}^2 &= \mathbb{E}\{\|\hat{v}_{i,f}\|^2\} - \sigma_{s,i}^2\\ &= \mathbb{E}\{\|\mathbf{t}_i^H\hat{\mathbf{R}}^{-1}\mathbf{y}_{c,f}\|^2\} - \sigma_{s,i}^2\\ &= \mathbf{t}_i^H\hat{\mathbf{R}}^{-1}\mathbb{E}\{\mathbf{y}_{c,f}\mathbf{y}_{c,f}^H\}\hat{\mathbf{R}}^{-1}\mathbf{t}_i - \sigma_{s,i}^2\\ &= \mathbf{t}_i^H\hat{\mathbf{R}}^{-1}\mathbf{t}_i - \sigma_{s,i}^2\\ &= \sigma_{s,i} - \sigma_{s,i}^2.\end{aligned} \tag{21}$$

Therefore, the SINR of the ith user at the output of MMSE estimator (input to the polar decoder) can be calculated as $\beta_i = \sigma_{s,i}/(1-\sigma_{s,i})$. Using the property $\text{vec}(\mathbf{A}_1\mathbf{A}_2\mathbf{A}_3) = (\mathbf{A}_3^T \otimes \mathbf{A}_1)\text{vec}(\mathbf{A}_2)$, we can write $\mathbf{t}_i$ in (14) as

$$\mathbf{t}_i = \mathbf{E}_i\mathbf{w}_c, \tag{22}$$

where $\mathbf{E}_i = \sqrt{P_c}\left(\text{diag}(\mathbf{b}_i) \otimes \mathbf{G}\text{diag}(\mathbf{h}_i)\right)$, and $\mathbf{w}_c = \text{vec}(\mathbf{W}_{c_s})$. Since $\sigma_{s,i} \leq 1$, we can see that β_i is an increasing function of $\sigma_{s,i}$. Therefore, in order to maximize the SINR, using (20) and (22), we maximize $\sigma_{s,i}$ by solving the following optimization problem

$$\begin{aligned}\hat{\mathbf{w}}_c = \arg&\max_{\mathbf{w}_c}\mathbf{w}_c^H\mathbf{C}_i\mathbf{w}_c\\ &\text{s.t.}\quad \left|[\mathbf{w}_c]_{(i,1)}\right| = 1,\end{aligned} \tag{23}$$

where

$$\mathbf{C}_i = \mathbf{E}_i^H\hat{\mathbf{R}}^{-1}\mathbf{E}_i. \tag{24}$$

Using the above discussion, we propose the following algorithm for the design of RIS phase-shifts:

1) Select an initial value $\mathbf{w}_c^{(0)}$.
2) Construct $\mathbf{C}_i^{(n)}$ according to (24), and obtain $\mathbf{q}_{i,\max}^{(n)}$,

where $\mathbf{q}_{i,\max}^{(n)}$ is the eigenvector of $\mathbf{C}_i^{(n)}$ corresponding to the largest eigenvalue [2].

3) $\mathbf{w}_c^{(n+1)} = \frac{1}{|\mathcal{S}_s|}\sum_{i\in\mathcal{S}_s}\mathbf{q}_{i,\max}^{(n)}$.
4) To apply the constraint in (23), every element of $\mathbf{w}_c^{(n+1)}$ is rescaled to have unit modulus.
5) Compute $g_n = \sum_{i\in\mathcal{S}_s}\mathbf{w}_c^{(n)H}\mathbf{C}_i^{(n)}\mathbf{w}_c^{(n)}$.
6) The algorithm is stopped in the nth iteration if $g_n < \frac{1}{N_s}\sum_{k=n-N_s}^{n-1} g_k$, where N_s is a design parameter; otherwise, set $n = n+1$ and go to step 2 for another iteration.

The algorithm declares $\mathbf{w}_c^{(m)}$ as the output, where $m = \arg\max_n g_n$. Note that in Step 3, we apply an ensemble average over vectors of different users to combine their results. Note that although the calculations in Sections III-B2 and III-B3 are based on the exact values of $\mathbf{h}_i$ and $\mathbf{b}_i$, we use their estimated values obtained by the JDCE algorithm since the exact ones are not known in practice.

IV. Numerical Results

In this section, we provide several numerical examples to demonstrate the performance of the proposed RIS-aided URA solution. In all the simulations, unless otherwise stated, we choose $\sigma_z^2 = -95$dBm, $B_c = 90$, $B_p = 10$, $S = 4$, $n_d = 256$, $n_s = 10$, $r = 16$, $L_G = 2$, $L_i = 2, i = 1, ..., K_a$, $M_1 = M_2 = N_1 = N_2 = 8$, $\alpha_1 = 1$, $N_s = 5$, $C_0 = 10^{-3}$, $\alpha_0 = 2.3$, and $d = \lambda/2$. The distances of each user-RIS path are drawn from $d_i \in U(200m, 300m)$, and it is set as $d_i = 100m$ for every RIS-BS path. We draw every element of $\mathbf{B}$, $\mathbf{P}$, and $\mathbf{W}_{p_s}$ with $\mathcal{CN}(0,1)$, then each element of $\mathbf{W}_{p_s}$ is rescaled to have unit modulus, every row of $\mathbf{B}$ is normalized to have a norm of n_s, and rows of $\mathbf{P}$ are scaled to satisfy $\|\mathbf{W}_{p_s}\text{diag}(\bar{\mathbf{p}}_i)\|^2 = \|\mathbf{W}_{p_s}\text{diag}(\bar{\mathbf{p}}_j)\|^2$, and $\frac{1}{2^{B_p}}\sum_{i=1}^{2^{B_p}}\|\bar{\mathbf{p}}_i\|^2 = n_p$ with $\bar{\mathbf{p}}_i$ being the ith row of $\mathbf{P}$. To construct the steering vectors of each path for the RIS in (1) and (3), we randomly choose $\bar{\phi}$ and $\bar{\psi}$ from $\mathcal{F}(N_1)$ and $\mathcal{F}(N_2)$, respectively, where $\mathcal{F}(.)$ is as defined in the last paragraph of the introduction section. Similarly, the AOAs of each received path to the BS are randomly selected from the sets $\mathcal{F}(M_1)$ and $\mathcal{F}(M_2)$. The PUPE of the system is defined as $P_e = p_{fa} + p_{md}$, where p_{md} is the probability that an active user's message is not decoded, and p_{fa} is the probability that a decoded message is not indeed sent. The efficiency of the JDCE in estimating CSI is evaluated by the normalized mean square error (NMSE) defined as

$$\frac{1}{K_a}\sum_{i=1}^{K_a}\mathbb{E}\left\{\frac{\|\hat{\mathbf{h}}_i - \mathbf{h}_i\|^2}{\|\mathbf{h}_i\|^2}\right\},$$

which can be estimated via Monte Carlo method.

To study the performance of the proposed JDCE scheme, we provide some specific results in Figs. 3 and 4 for different values of n_p and P_p such that n_pP_p is kept constant. Specifically, we plot the NMSE and the detection probability p_d, i.e., the probability that an active pilot is detected by JDCE. Note that for computing the NMSE, we only consider the channel coefficients of the detected pilots that are picked only by one user (no collision case). It is observed that despite the constant energy, the performance of the proposed JDCE is improved by increasing n_p. However, increasing n_p can decrease the efficiency of the URA system. Thus, this parameter must be suitably selected.

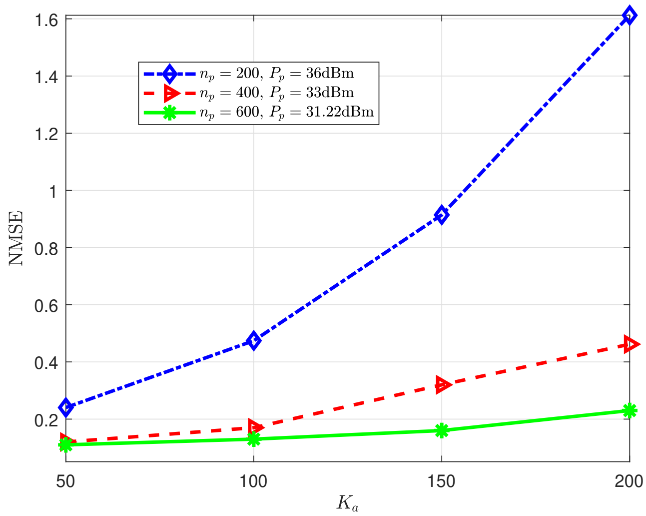

Fig. 3: The NMSE of the JDCE for a fixed P_pn_p, and different values of n_p and P_p.

In Fig. 5, we depict the average transmit power required by the proposed decoder to achieve the target PUPE of 0.1 for $n_s = 10$, $n_d = 256$, and different RIS design strategies. Note that the simulations are run based on a known CSI. We can deduce from this figure that the proposed beamforming strategy performs better than the strategy employed in [11] and the case of randomly generated phase-shifts (resulting in up to 11dBm and 17dBm power savings). This improvement is due to the employment of a more suitable metric in the RIS design of the proposed algorithm, where the overall phase-shift matrix is obtained by minimizing the decoding error probability. However, the RIS design algorithm in [11] maximizes the minimum channel gain among active users. Note that since we consider the direct link between each user and the BS to be completely blocked, no communication is possible without the help of RIS.

V. Conclusions

We have proposed a RIS-aided URA scheme to enable connectivity between the BS and the users whose direct channel to the BS is blocked. The proposed scheme operates in two phases, the RIS configuration phase and the data phase. In the former, transmitted pilots are identified in the presence of heavy interference, their corresponding CSI is estimated, and RIS reflection coefficients are suitably devised. In the data phase, a decoder detects the transmitted messages using a polar list decoder, and the contribution of successfully decoded messages is removed from the received signal using successive interference cancellation. We have shown that the proposed RIS-aided URA scheme

[2]For a Hermitian matrix $\mathbf{C}$ and a vector with unit norm, $\|\mathbf{w}\|^2 = 1$, the maximum value of $c = \mathbf{w}^H\mathbf{C}\mathbf{w}$ is obtained by choosing $\mathbf{w}$ as the eigenvector of $\mathbf{C}$ corresponding to its largest eigenvalue [23].

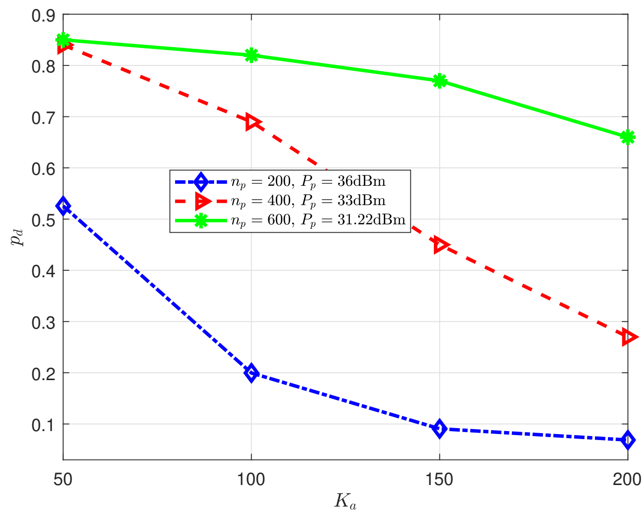

Fig. 4: The detection probability of the JDCE for a fixed $P_p n_p$, and different values of n_p and P_p.

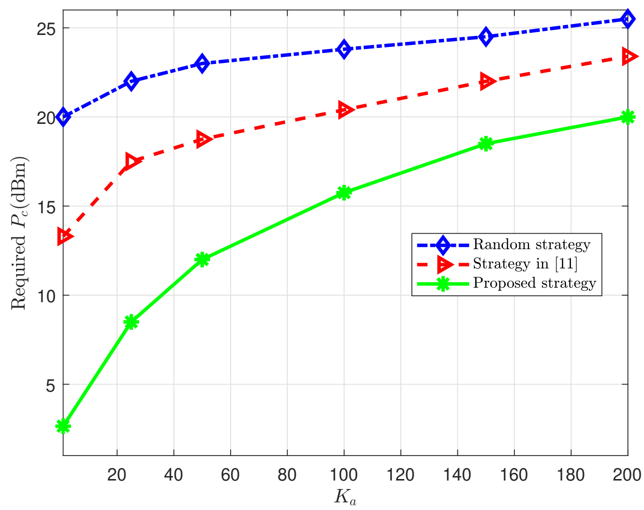

Fig. 5: The required P_c to achieve the target PUPE of 0.1 for $n_s = 10$, $n_d = 256$, and different RIS phase-shift strategies.

performs well in the URA scenario where the direct link between the users and the BS is obstructed.

REFERENCES

[1] Y. Polyanskiy, "A perspective on massive random-access," in *Proc. IEEE Int. Symp. Inf. Theory (ISIT)*, Aachen, Germany, June 2017, pp. 2523–2527.

[2] A. K. Tanc and T. M. Duman, "Massive random access with trellis based codes and random signatures," *IEEE Commun. Lett.*, vol. 25, no. 5, pp. 1496–1499, May 2021.

[3] A. K. Pradhan, V. K. Amalladinne, K. R. Narayanan, and J.-F. Chamberland, "Polar coding and random spreading for unsourced multiple access," in *Proc. IEEE Int. Conf. Commun. (ICC)*, Dublin, Ireland, June 2020, pp. 1–6.

[4] M. J. Ahmadi and T. M. Duman, "Random spreading for unsourced MAC with power diversity," *IEEE Commun. Lett.*, vol. 25, no. 12, pp. 3995–3999, Dec. 2021.

[5] M. J. Ahmadi and T. M. Duman, "Unsourced random access with a massive MIMO receiver using multiple stages of orthogonal pilots," in *Proc. IEEE Int. Symp. Inf. Theory (ISIT)*, Espoo, Finland, July 2022, pp. 2880-2885.

[6] M. J. Ahmadi, M. Kazemi, and T. M. Duman, "Unsourced random access with a massive MIMO receiver using multiple stages of orthogonal pilots: MIMO and single-antenna structures," *IEEE Trans. Wireless Commun.*, June 2023.

[7] M. Ozates and T. M. Duman, "Unsourced random access over frequency-selective channels," *IEEE Commun. Lett.*, vol. 27, no. 4, pp. 1230–1234, Apr. 2023.

[8] M. Ozates, M. Kazemi and T. M. Duman, "A slotted unsourced random access scheme with a massive MIMO receiver," in *Proc. IEEE Global Commun. Conf. (GLOBECOM)*, Rio de Janeiro, Brazil, Jan. 2022, pp. 2456–2461.

[9] W. Yan, X. Yuan, Z. -Q. He and X. Kuai, "Passive beamforming and information transfer design for reconfigurable intelligent surfaces aided multiuser MIMO systems," *IEEE J. Select. Areas Commun.*, vol. 38, no. 8, pp. 1793–1808, Aug. 2020.

[10] H. Shen, W. Xu, S. Gong, Z. He and C. Zhao, "Secrecy rate maximization for intelligent reflecting surface assisted multi-antenna communications," *IEEE Commun. Lett.*, vol. 23, no. 9, pp. 1488–1492, Sept. 2019.

[11] X. Shao, L. Cheng, X. Chen, C. Huang and D. W. K. Ng, "Reconfigurable intelligent surface-aided 6G massive access: coupled tensor modeling and sparse bayesian learning," *IEEE Trans. Wireless Commun.*, vol. 21, no. 12, pp. 10145–10161, Dec. 2022.

[12] F. Laue, V. Jamali and R. Schober, "IRS-assisted active device detection," in *Proc. IEEE Workshop Signal Process. Adv. Wireless Commun. (SPAWC)*, Lucca, Italy, Sep. 2021, pp. 556–560.

[13] C. Huang, A. Zappone, G. C. Alexandropoulos, M. Debbah and C. Yuen, "Reconfigurable intelligent surfaces for energy efficiency in wireless communication," *IEEE Trans. Wireless Commun.*, vol. 18, no. 8, pp. 4157–4170, June 2019.

[14] Q. Wu and R. Zhang, "Intelligent reflecting surface enhanced wireless network via joint active and passive beamforming," *IEEE Trans. Wireless Commun.*, vol. 18, no. 11, pp. 5394–5409, Nov. 2019.

[15] A. L. Swindlehurst, G. Zhou, R. Liu, C. Pan and M. Li, "Channel estimation with reconfigurable intelligent surfaces—a general framework," *Proc. IEEE*, vol. 110, no. 9, pp. 1312–1338, Sep. 2022.

[16] X. Wei, D. Shen and L. Dai, "Channel estimation for RIS assisted wireless communications—part II: an improved solution based on double-structured sparsity," *IEEE Commun. Lett.*, vol. 25, no. 5, pp. 1403–1407, May 2021.

[17] C. Hu, L. Dai, S. Han and X. Wang, "Two-timescale channel estimation for reconfigurable intelligent surface aided wireless communications," *IEEE Trans. Commun.*, vol. 69, no. 11, pp. 7736–7747, Nov. 2021.

[18] C. Ruan, Z. Zhang, H. Jiang, J. Dang, L. Wu and H. Zhang, "Approximate message passing for channel estimation in reconfigurable intelligent surface aided MIMO multiuser systems," *IEEE Trans. Commun.*, vol. 70, no. 8, pp. 5469–5481, Aug. 2022.

[19] H. Guo and V. K. N. Lau, "Uplink cascaded channel estimation for intelligent reflecting surface assisted multiuser MISO systems," *IEEE Trans. Signal Process.*, vol. 70, no. , pp. 3964–3977, Nov. 2022.

[20] Z. Mao, X. Liu and M. Peng, "Channel estimation for intelligent reflecting surface assisted massive MIMO systems—a deep learning approach," *IEEE Commun. Lett.*, vol. 26, no. 4, pp. 798–802, April 2022.

[21] X. Shi, J. Wang and J. Song, "Triple-structured compressive sensing-based channel estimation for RIS-aided MU-MIMO systems," *IEEE Trans. Wireless Commun.*, vol. 21, no. 12, pp. 11095–11109, Dec. 2022.

[22] Q. Wu and R. Zhang, "Beamforming optimization for wireless network aided by intelligent reflecting surface with discrete phase-shifts," *IEEE Trans. Commun.*, vol. 68, no. 3, pp. 1838–1851, March 2020.

[23] K. M. Hoffman and R. Kunze, Linear algebra. Englewood Cliffs, NJ, USA: Prentice-Hall, 1971.